MEDICAL SCIENCE MONITOR

CLINICAL RESEARCH

e-ISSN 1643-3750
© Med Sci Monit, 2015; 21: 1781-1791
DOI: 10.12659/MSM.894669

Received: 2015.05.15
Accepted: 2015.05.28
Published: 2015.06.20

Comparative Metabolomic Profiling of Hepatocellular Carcinoma Cells Treated with Sorafenib Monotherapy *vs.* Sorafenib-Everolimus Combination Therapy

Authors' Contribution:
Study Design A
Data Collection B
Statistical Analysis C
Data Interpretation D
Manuscript Preparation E
Literature Search F
Funds Collection G

AEF 1 **Jian-feng Zheng***
BC 2 **Juan Lu***
DF 1 **Xiao-zhong Wang**
AFG 1 **Wu-hua Guo**
AEG 1,3 **Ji-xiang Zhang**

1 The Second Affiliated Hospital of Nanchang University, Nanchang, Jiangxi, P.R. China
2 Jiangxi Children's Hospital, Nanchang, Jiangxi, P.R. China
3 Jiangxi Province Key Laboratory of Molecular Medicine, Nanchang, Jiangxi, P.R. China

* These authors contributed equally

Corresponding Authors: Ji-xiang Zhang, e-mail: jixiangzhang123@163.com or jixiangz@tom.com, Wu-hua Guo, e-mail: guowuhua@aliyun.com
Source of support: This work was supported in part by the National Natural Science Foundation of China (grant numbers 81360363, 81360074, 81260360) and the Educational Commission of Jiangxi Province of China (grant number GJJ13171)

Background: Sorafenib-everolimus combination therapy may be more effective than sorafenib monotherapy for hepatocellular carcinoma (HCC). To better understand this effect, we comparatively profiled the metabolite composition of HepG2 cells treated with sorafenib, everolimus, and sorafenib-everolimus combination therapy.

Material/Methods: A 2D HRMAS ^{1}H-NMR metabolomic approach was applied to identify the key differential metabolites in 3 experimental groups: sorafenib (5 μM), everolimus (5 μM), and combination therapy (5 μM sorafenib +5 μM everolimus). MetaboAnalyst 3.0 was used to perform pathway analysis.

Results: All OPLS-DA models displayed good separation between experimental groups, high-quality goodness of fit (R2), and high-quality goodness of predication (Q2). Sorafenib and everolimus have differential effects with respect to amino acid, methane, pyruvate, pyrimidine, aminoacyl-tRNA biosynthesis, and glycerophospholipid metabolism. The addition of everolimus to sorafenib resulted in differential effects with respect to pyruvate, amino acid, methane, glyoxylate and dicarboxylate, glycolysis or gluconeogenesis, glycerophospholipid, and purine metabolism.

Conclusions: Sorafenib and everolimus have differential effects on HepG2 cells. Sorafenib preferentially affects glycerophospholipid and purine metabolism, while the addition of everolimus preferentially affects pyruvate, amino acid, and glucose metabolism. This phenomenon may explain (in part) the synergistic effects of sorafenib-everolimus combination therapy observed *in vivo*.

MeSH Keywords: **Carcinoma, Hepatocellular • Hep G2 Cells • Metabolomics**

Full-text PDF: http://www.medscimonit.com/abstract/index/idArt/894669

2803 3 6 19

Indexed in: [Current Contents/Clinical Medicine] [SCI Expanded] [ISI Alerting System] [ISI Journals Master List] [Index Medicus/MEDLINE] [EMBASE/Excerpta Medica] [Chemical Abstracts/CAS] [Index Copernicus]

Background

Hepatocellular carcinoma (HCC) is one of the most common malignancies and causes approximately 600 000 fatalities worldwide annually [1]. The only currently approved systemic therapy for advanced HCC is sorafenib (Nexavar®), an oral multi-kinase inhibitor that blocks tumor cell proliferation through targeting Raf/MEK/ERK signaling [1]. However, clinical evidence suggests that sorafenib combined with a mammalian target of rapamycin (mTOR) inhibitor may be a more effective and tolerable treatment strategy for advanced HCC [2].

Metabolomics – the study of biological systems that assesses changes in metabolites after a specific stimulation or interference – has provided valuable insights by focusing on the metabolite end-products affected by drugs. With respect to HCC, several previous metabolomics studies have analyzed the metabolic responses of HCC cells to various chemotherapeutics [3–5]. Zhou et al. employed a metabolomics approach to assess the effects of sorafenib monotherapy on the HCC cell line HepG2 that revealed significant changes to several metabolic pathways in a concentration-dependent manner [6].

Although Zhou et al. study demonstrated profound dose-dependent metabolic changes in HepG2 cells after sorafenib monotherapy, there has been no metabolomic study to date that has comparatively profiled the metabolite composition of HCC cells treated by a combination of sorafenib and a mTOR inhibitor. Specifically, everolimus (40-O-(2-hydroxyethyl)-rapamycin, RAD001/Afinitor®) is the only mTOR inhibitor currently under investigation for HCC [7,8], and there is clinical evidence suggesting that sorafenib-everolimus combination therapy is more effective than sorafenib monotherapy [2].

Therefore, the objective of this metabolomic study was to comparatively profile the metabolite composition of HepG2 cells treated with sorafenib monotherapy, everolimus monotherapy, and sorafenib-everolimus combination therapy using a 2D HRMAS ^{1}H-NMR metabolomic approach.

Material and Methods

Material and cell lines

High-glucose DMEM, fetal calf serum (FCS), penicillin–streptomycin, trypsin and EDTA were obtained from Thermo (Beijing, China), and the human HCC cell line HepG2 was acquired from Shanghai Institutes for Biological Sciences at the Chinese Academy of Sciences (Shanghai, China) [9]. As previously described [9], the HepG2 cells were maintained in high-glucose DMEM supplemented with 10% heat-inactivated (56°C, 30 min) FCS, penicillin (100 U/ml), and streptomycin (100 µg/ml) at 37°C in a humidified atmosphere of 5% CO_2 with passage every 3 days.

MTT cytotoxicity sssay

The MTT assay was performed as previously described with slight modifications [9,10]. Briefly, 3-(4,5-Dimethyl-thiagol-2yl)-2,5-diplenyltertrazollium (MTT) was obtained from Solarbio Science & Technology Co., Ltd. (Beijing, China). HepG2 cells were seeded onto 96-well plates (1×10^4 cells/well) and cultured overnight before drug treatment. Culture medium containing 6 concentrations of sorafenib (0.00 [control], 1.25, 2.5, 5, 10, and 20 µM by serial dilution) and 6 concentrations of everolimus (0.00 [control], 1.25, 2.5, 5, 10, and 20 µM by serial dilution) with 0.1% dimethylsulfoxide (DMSO) was added into 96-well cell culture plates and incubated for 48 h. After 48 h, MTT dissolved in phosphate-buffered saline (PBS, 0.5 mg/ml) was added to each well and incubated for 4 h. Absorbance was determined at 570 nm by addition of 100 µl DMSO for each well using an enzyme-linked immunosorbent assay (ELISA) reader. The procedure was carried in triplicate.

Annexin V-FITC staining for apoptosis

Apoptosis was quantified using flow cytometry to measure the levels of detectable phosphatidylserine on the outer membrane of apoptotic cells as previously described with slight modifications [9]. HepG2 cells (4×10^5 cells/ml) were seeded onto 96-well plates and incubated with 6 concentrations of sorafenib (0.00 [control], 1.25, 2.5, 5, 10, and 20 µM by serial dilution) and 6 concentrations of everolimus (0.00 [control], 1.25, 2.5, 5, 10, and 20 µM by serial dilution) with 0.1% DMSO for 48 h. Then, the cells were harvested by trypsinization, washed in ice-cold PBS, and re-suspended in diluted binding buffer from the Annexin V-FITC kit (Bestbio Inc., Shanghai, China) based on the manufacturer's instructions. The procedure was carried out in triplicate.

Cell cycle analysis

Cell cycle phase distribution was analyzed by a cell cycle analysis kit (Beyotime Institute of Biotechnology, Jiangsu, China) as previously described, with slight modifications [9]. Briefly, HepG2 cells were treated with 6 concentrations of sorafenib (0.00 [control], 1.25, 2.5, 5, 10, and 20 µM by serial dilution) and 6 concentrations of everolimus (0.00 [control], 1.25, 2.5, 5, 10, and 20 µM by serial dilution) with 0.1% DMSO for 48 h. Then, the cells were harvested by trypsinization, washed in ice-cold PBS, and fixed in 70% ice-cold ethanol overnight. Subsequently, the fixed cells were washed with ice-cold PBS before incubation with the binding buffer containing RNase and propidium iodide for 30 min at 37°C in the dark. Finally, the stained cells were analyzed by flow cytometry with Modfit LT 4.0.The procedure was carried out in triplicate.

Indexed in: [Current Contents/Clinical Medicine] [SCI Expanded] [ISI Alerting System] [ISI Journals Master List] [Index Medicus/MEDLINE] [EMBASE/Excerpta Medica] [Chemical Abstracts/CAS] [Index Copernicus]

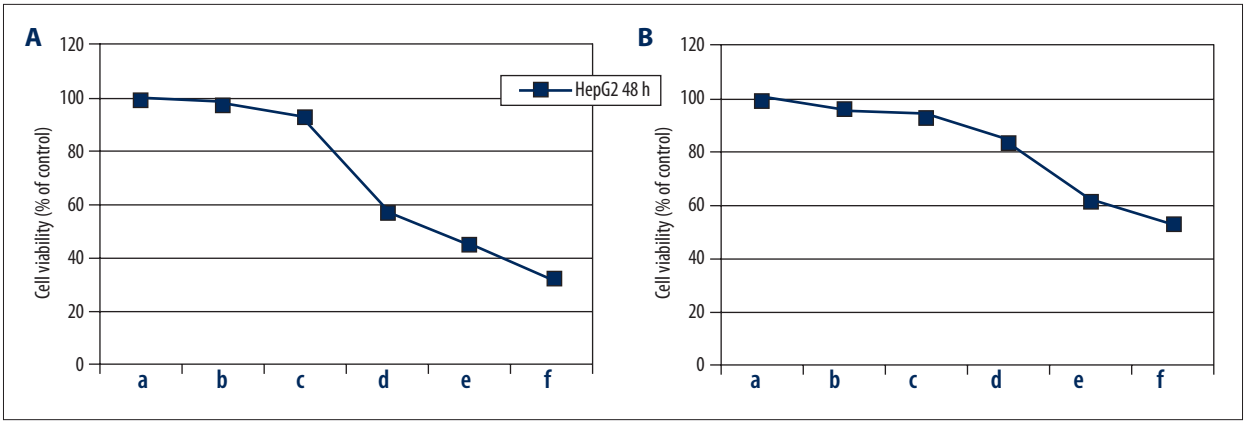

Supplementary Figure 1. MTT cytotoxicity assays for sorafenib monotherapy and everolimus monotherapy. Cell viability of HepG2 cells treated with (**A**) sorafenib monotherapy and (**B**) everolimus monotherapy. Dosages: (**a**) 0.00 μmol/l, (**b**) 1.25 μmol/l, (**c**) 2.5 μmol/l, (**d**) 5 μmol/l, (**e**) 10 μmol/l, and (**f**) 20 μmol/l.

2D HRMAS ^{1}H-NMR metabolomic analysis

This metabolomic analysis was evaluated as previously described, with slight modifications [3]. HepG2 cells (~3×10^6 cells/well) were seeded onto 96-well cell culture plates and cultured overnight. Based on the aforementioned cytotoxicity, apoptosis, and cell cycle monotherapy data, 3 separate treatment regimens – 5 μM sorafenib, 5 μM everolimus, and 5 μM sorafenib +5 μM everolimus – with 0.1% DMSO were added to the cells and incubated for 48 h. At 48 h, erythrosine was used to assess cell viability. Cells underwent trypsin digestion and were then twice rinsed with PBS-D_2O (9.6 mg/ml PBS in D_2O) (J&K, China). These cell pellets were refrigerated at –80°C.

All of the following steps were performed in an ice-cold environment. The cell pellets were re-suspended in 2 ml of methanol/chloroform (2:1, v/v). The cells were then ultrasonicated for a period of 1 min. Then, we added 500 μl of H_2O/chloroform (1:1, v/v) to each cell suspension and centrifuged the suspensions at 1500 g for 20 min at 4°C. We evaporated both the aqueous phases and precipitates under argon flux. This was followed by lyophilization and refrigeration at –80°C.

Both phases were dissolved in PBS-D_2O with the pH adjusted to 7.20. The sodium salt of 3-(trimethylsilyl)-1-propanesulfonic acid (1% in D_2O) was used as the internal standard. $CDCl_3$/CD_3OD (2:1, v/v; SDS, Peypin, France) was used to recover the organic phase. A 500-MHz BrukerAvance DRX spectrometer with an HRMAS probe was used. Water-soluble extracts (50 μl), protein extracts (50 μl), and unprocessed cell pellets (5–10×10^6 cells/pellet) were placed into rotor tubes, which underwent spinning at 4 kHz. The tubes were then cooled to 4°C.

A nuclear Overhauser enhancement spectroscopy sequence with low-power water-signal presaturation was used to obtain 1D 1H-NMR spectra with a relaxation delay of 3.8 s and a sequence mixing time of 100 ms. A 170-sec acquisition duration resulted from a 12-ppm spectral width with 32 transients and 16384 complex data points. A spline function was used for baseline correction after Fourier transformation.

A total correlation spectroscopy sequence was used to obtain 2D ^{1}H-NMR spectra. The following setting were applied: low-power water signal suppression, spectral bandwidth of 6 ppm along both frequency axes, 256 samples in the first axis, 2048 samples in the second axis, mixing time of 75 ms with spin-lock pulse train, relaxation delay of 1 s, and 16 repetitions. The 2D spectral acquisition duration was 101 min. We also performed a second 1D ^{1}H-NMR spectral acquisition. We reconstructed the spectra at a 2048×256 resolution for assignment and a 256×256 resolution for quantification. A second-order polynomial was used for baseline correction. 2D spectral data were used to calculate cross-peak volumes.

Multivariate statistical analysis

The integral values of samples were imported into SIMCA-P+ 12.0. OPLS-DA was applied to the unit variance (UV)-scaled spectral data to visualize discrimination between the HepG2 cells treated with different drug treatments [11]. The coefficient loading plots of the OPLS-DA model were used to identify the spectral variables responsible for sample differentiation on the scores plot [12]. Based on the number of samples used to construct the OPLS-DA models, a correlation coefficient of $|r|>0.226$ (equivalent to a p-value of less than 0.05) was adopted as the cut-off value. The metabolites with correlation coefficients of $|r|>0.226$ were identified as the key metabolites responsible for sample differentiation in the three comparisons. A 199-iteration permutation test was performed to rule-out non-random separation between groups. If the Q^2 and R^2values resulting from the original model were higher than the corresponding values from the permutation test, the model was deemed valid [13].

Indexed in: [Current Contents/Clinical Medicine] [SCI Expanded] [ISI Alerting System] [ISI Journals Master List] [Index Medicus/MEDLINE] [EMBASE/Excerpta Medica] [Chemical Abstracts/CAS] [Index Copernicus]

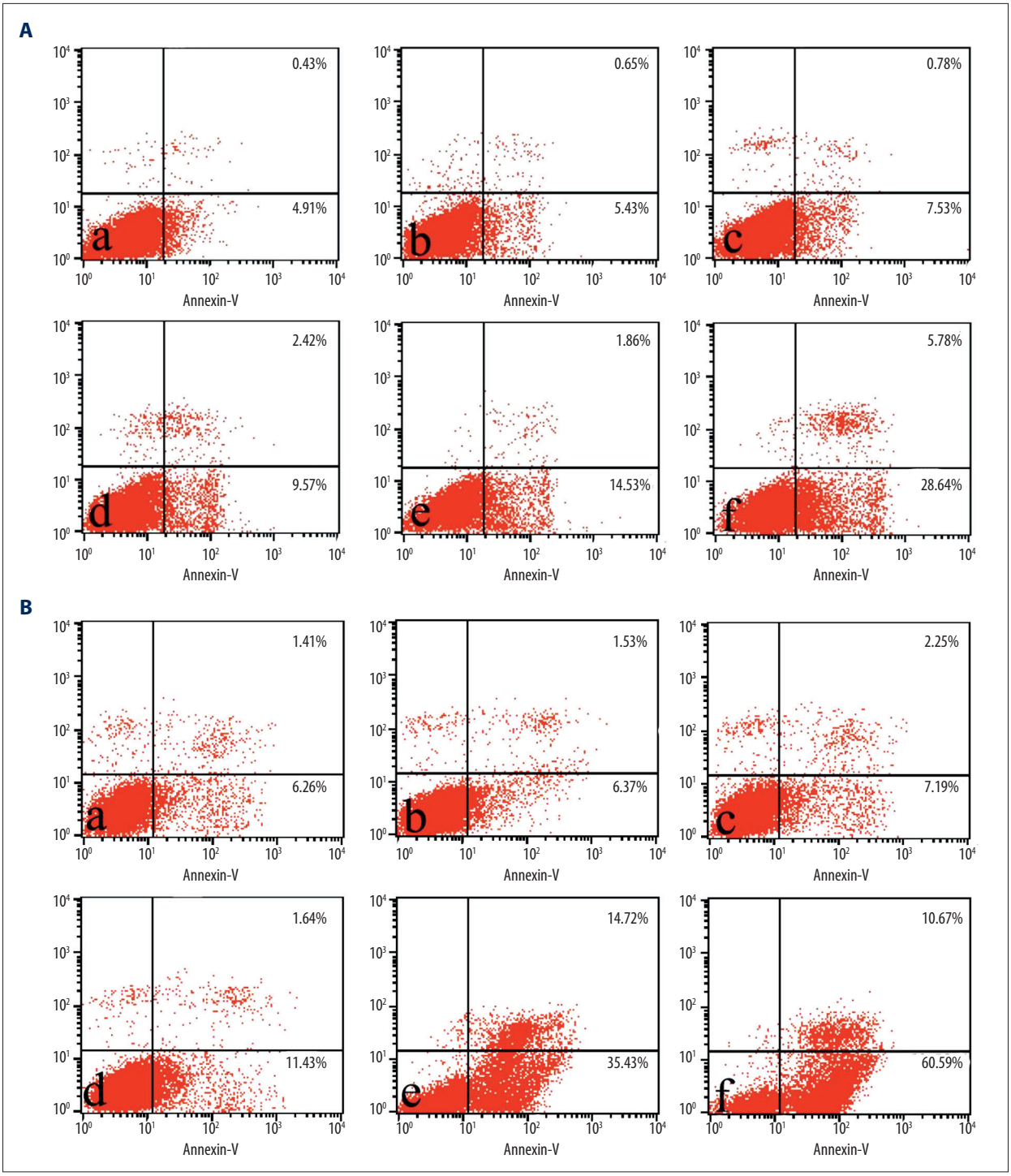

Supplementary Figure 2. Apoptosis assays for sorafenib monotherapy and everolimus monotherapy. Annexin V-FITC flow cytometry findings for (**A**) sorafenib monotherapy and (**B**) everolimus monotherapy. Dosages: (**a**) 0.00 μmol/l, (**b**) 1.25 μmol/l, (**c**) 2.5 μmol/l, (**d**) 5 μmol/l, (**e**) 10 μmol/l, and (**f**) 20 μmol/l.

Pathway analysis

MetaboAnalyst 3.0 was used to identify the metabolic pathways more likely to be linked with the metabolic alterations induced under the 3 treatment comparisons [14]. The differential metabolites from each comparison were uploaded to the Pathway Analysis functionality on the MetaboAnalyst website (*http://www.metaboanalyst.ca/*). The Homo sapiens pathway

Indexed in: [Current Contents/Clinical Medicine] [SCI Expanded] [ISI Alerting System] [ISI Journals Master List] [Index Medicus/MEDLINE] [EMBASE/Excerpta Medica] [Chemical Abstracts/CAS] [Index Copernicus]

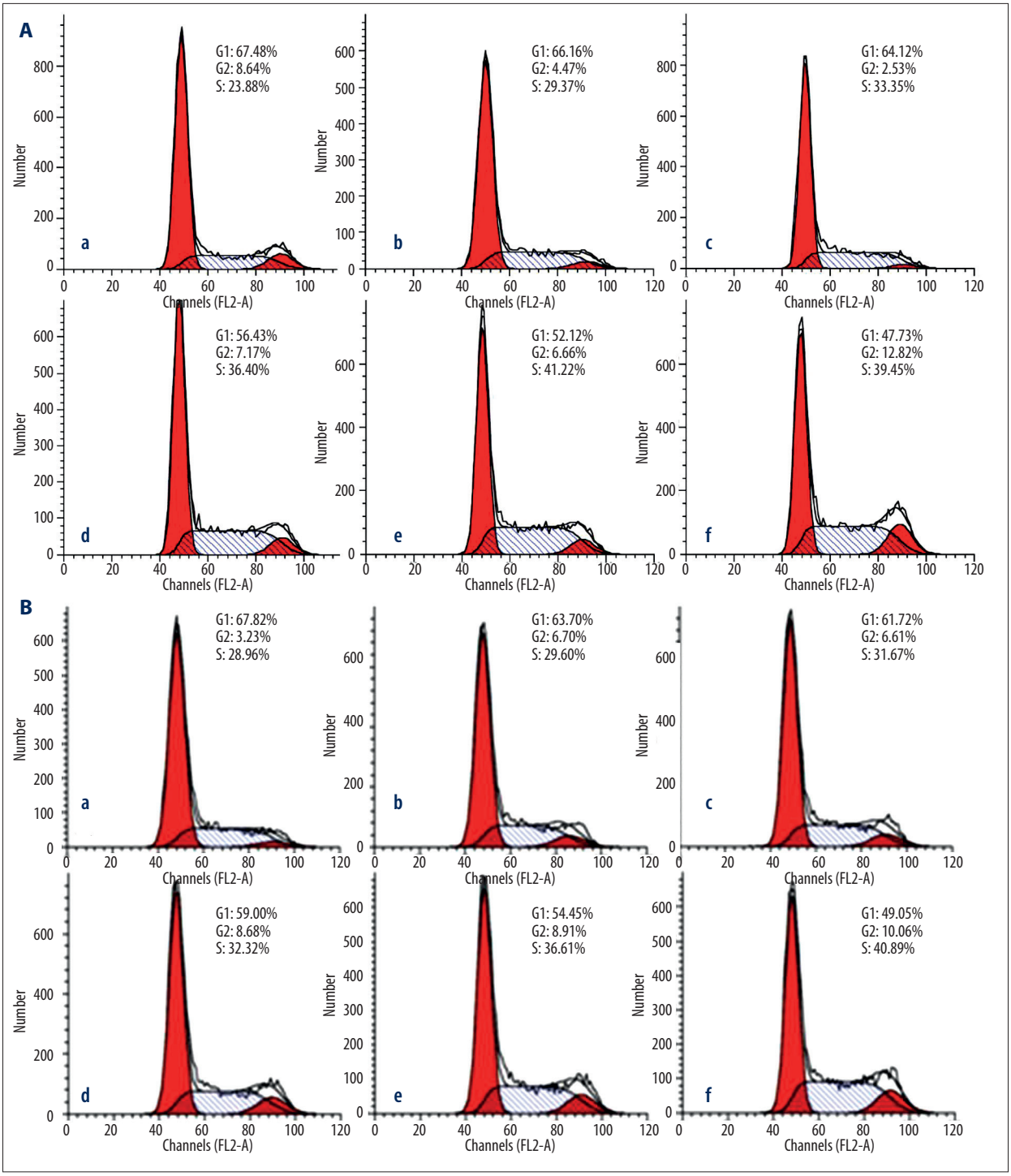

Supplementary Figure 3. Cell cycle assays for sorafenib monotherapy and everolimus monotherapy. Cell cycle phase distributions for (**A**) sorafenib monotherapy and (**B**) everolimus monotherapy. Dosages: (**a**) 0.00 μmol/l, (**b**) 1.25 μmol/l, (**c**) 2.5 μmol/l, (**d**) 5 μmol/l, (**e**) 10 μmol/l, and (**f**) 20 μmol/l.

library was used. The reference metabolome included all compounds in the selected pathways. The following pathway analysis algorithms were selected: hypergeometric test for over-representation analysis and relative-betweenness centrality for pathway topology analysis.

Indexed in: [Current Contents/Clinical Medicine] [SCI Expanded] [ISI Alerting System] [ISI Journals Master List] [Index Medicus/MEDLINE] [EMBASE/Excerpta Medica] [Chemical Abstracts/CAS] [Index Copernicus]

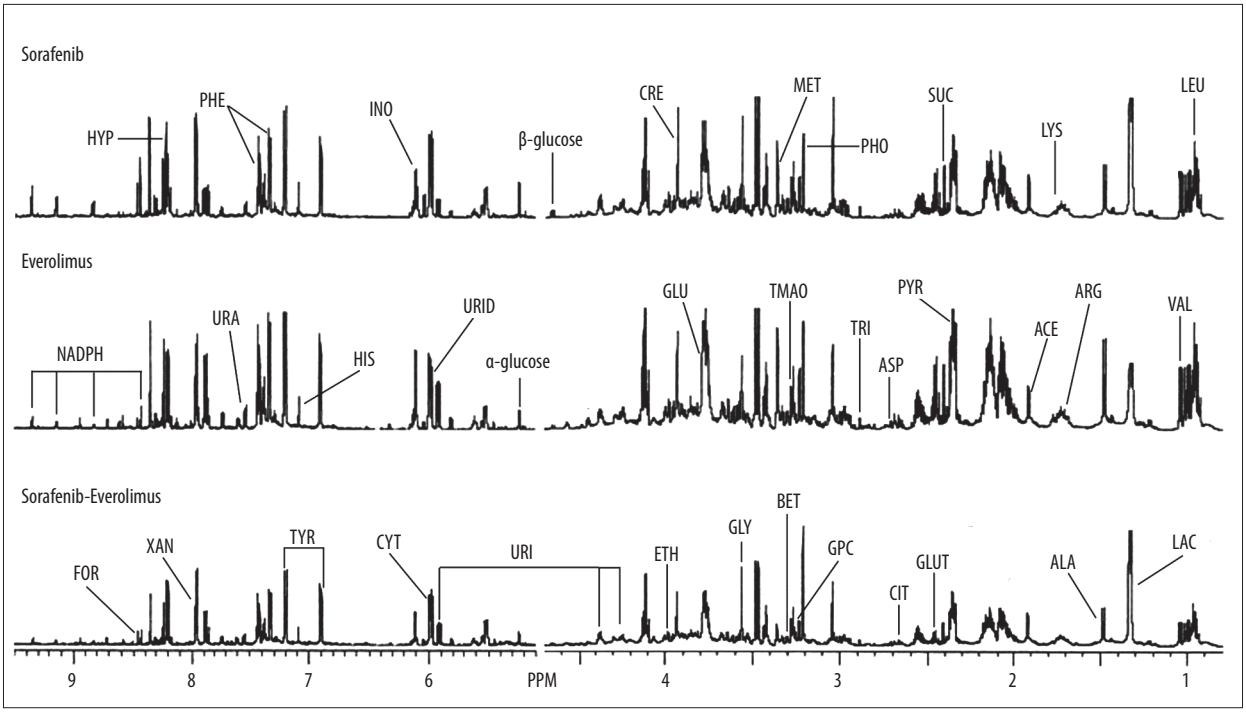

Figure 1. Representative NMR Spectra. Representative NMR spectra of HepG2 cells treated with sorafenib monotherapy (5 μM sorafenib), everolimus monotherapy (5 μM everolimus), and sorafenib-everolimus combination therapy (5 μM sorafenib +5 μM everolimus). LEU – leucine; VAL – valine; LAC – lactate; ALA – alanine; LYS – lysine; ARG – arginine; ACE – acetate; GLUT – glutamine; PYR – pyruvate; SUC – succinate; CIT – citrate; BET – betaine; GLY – glycine; URA – uracil; TYR – tyrosine; HIS – histidine; PHE – phenylalanine; FOR – formate; TRI – trimethylamine; GLU – glutathione disulfide; ASP – aspartate; CRE – creatine; PHO – phosphorylcholine; GPC – glycerophosphorylcholine; MET – methanol; URI – uridine; INO – inosine; CYT – cytidine; URID – uridine diphosphate; XAN – xanthine; HYP – hypoxanthine; NADP – nicotinamide adenine dinucleotide phosphate; TMAO – trimethyl amino oxide; ETH – ethanolamine.

Results

Dose selection based on cytotoxicity, apoptosis, and cell cycle findings

The MTT cytotoxicity data revealed clear inflection points in cell viability at ~5 μM sorafenib (Supplementary Figure 1A) and ~5 μM everolimus (Supplementary Figure 1B). The apoptosis data revealed clear inflection points in apoptosis rates at 10–20 μM sorafenib (Supplementary Figure 2A) and 5–10 μM everolimus (Supplementary Figure 2B). The cell cycle phase distribution data did not reveal any significant inflection points with respect to sorafenib or everolimus dosage (Supplementary Figure 3). From this data, we created 3 experimental groups for metabolomic comparison: sorafenib monotherapy (5 μM), everolimus monotherapy (5 μM), and combination therapy (5 μM sorafenib +5 μM everolimus).

NMR spectra and OPLS-DA modeling

The representative spectra from the 2D HRMAS ^{1}H-NMR metabolomic analysis of these 3 experimental groups are provided in Figure 1. The metabolite resonances were assigned based on previous literature and the 2D NMR results. Spectra from all 3 groups were dominated by numerous signals from low-molecular mass metabolites (Figure 1).

OPLS-DA models derived from the ^{1}H-NMR data were then constructed to maximize the discrimination between groups and to focus on the metabolic variations that significantly contributed to classifications. Three OPLS-DA models were constructed for 3 comparisons: (i) sorafenib monotherapy (5 μM) *vs.* everolimus monotherapy (5 μM) (Figure 2A), (ii) sorafenib monotherapy (5 μM) *vs.* combination therapy (5 μM sorafenib +5 μM everolimus) (Figure 2B), and (iii) everolimus monotherapy (5 μM) *vs.* combination therapy (5 μM sorafenib + 5 μM everolimus) (Figure 2C). All 3 OPLS-DA models displayed good separation between the experimental groups, high-quality goodness of fit (R2), and high-quality goodness of predication (Q2) (Figure 2).

Identification of key differential metabolites

The coefficient loading plots of the 3 OPLS-DA models were used to identify the metabolites responsible for sample differentiation on the scores plots. First, the metabolite profiles

Indexed in: [Current Contents/Clinical Medicine] [SCI Expanded] [ISI Alerting System] [ISI Journals Master List] [Index Medicus/MEDLINE] [EMBASE/Excerpta Medica] [Chemical Abstracts/CAS] [Index Copernicus]

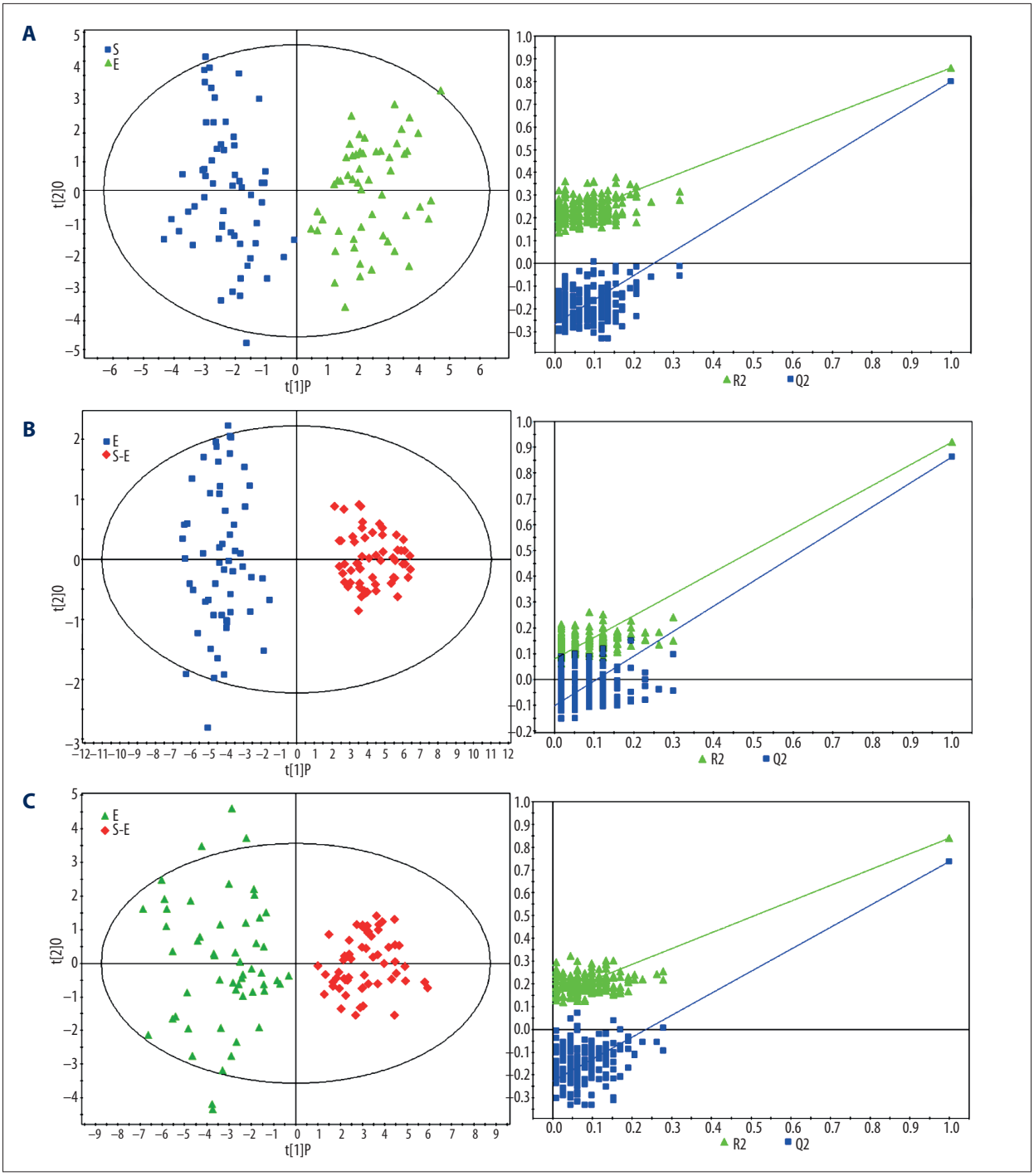

Figure 2. OPLS-DA score plots. (**A**) OPLS-DA score plots showing a clear discrimination between HepG2 cells treated with sorafenib (blue squares) and HepG2 cells treated with everolimus (green triangles). A 199-iteration permutation test showing the original $R^2$and Q^2values (R^2=0.860, Q^2=0.802) as significantly higher than corresponding permuted values (bottom left), which demonstrates the OPLS-DA model's robustness. (**B**) OPLS-DA score plots showing a clear discrimination between HepG2 cells treated with sorafenib (blue squares) and HepG2 cells treated with sorafenib-everolimus (red diamonds). A 199-iteration permutation test showing the original $R^2$and Q^2values (R^2=0.929, Q^2=0.879) as significantly higher than corresponding permuted values (bottom left), which demonstrates the OPLS-DA model's robustness. (**C**) OPLS-DA score plots showing a clear discrimination between HepG2cells treated with everolimus (green triangles) and HepG2cells treated with sorafenib-everolimus (red diamonds). A 199-iteration permutation test showed the original $R^2$and Q^2values (R^2=0.841, Q^2=0.748) as significantly higher than corresponding permuted values (bottom left), which demonstrates the OPLS-DA model's robustness.

Indexed in: [Current Contents/Clinical Medicine] [SCI Expanded] [ISI Alerting System] [ISI Journals Master List] [Index Medicus/MEDLINE] [EMBASE/Excerpta Medica] [Chemical Abstracts/CAS] [Index Copernicus]

Table 1. Key metabolites responsible for discrimination between sorafenib monotherapy and everolimus monotherapy.

No.	Chemical shift/ppm multiplicity*	Metabolites	r**	*P*-value***
1	1.33(d), 4.11(q)	Lactate	–0.321	1.286E-4
2	1.48(d), 3.78(q)	Alanine	–0.288	4.569E-11
3	1.73(m), 1.93(m), 3.75(t)	Arginine	–0.994	1.865E-16
4	5.81(d), 7.54(d)	Uracil	0.233	7.532E-6
5	3.57(s)	Glycine	–0.486	3.629E-13
6	3.81(d), 4.14(q), 4.24(t), 5.90(d)	Uridine	0.255	5.239 E-1
7	8.46(s)	Formate	–0.464	1.886E-14
8	3.23(s), 3.68(t), 4.32(t)	Glycerophosphorylcholine	0.391	8.364 E-1
9	3.22(s), 3.61(t), 4.19(t)	Phosphorylcholine	–0.303	8.728E-5
10	2.97(dd), 3.31(dd), 4.76(t)	Glutathionedisulfide	0.391	5.432 E-1
11	7.9(s)	Xanthine	–0.754	3.258E-17
12	2.68(m), 2.82(m), 3.91(m)	Aspartate	0.435	9.482 E-1

* Multiplicity: s – singlet; d – doublet; t – triplet; q – quartet; dd – doublet of doublets; m – multiplet. ** Correlation coefficient was obtained from OPLS-DA with a threshold of 0.226. Positive values indicate higher levels with everolimus treatment, and negative values indicate lower levels with everolimus treatment. *** *P*-values were derived from a non-parametric Mann-Whitney U test. The *p*-values of some main metabolites were not significantly perturbed in the univariate statistical analysis. But the OPLS-DA model showed that the addition of these metabolites resulted in the highest discrimination power. This result shows the advantage of a multivariate statistical approach in detecting the potential significance of subtle metabolic differences between experimental groups related to an associated univariate analysis.

of sorafenib-treated HepG2 cells were markedly differentiated from everolimus-treated HepG2 cells (Table 1). Five small molecules (uracil, uridine, glycerophosphorylcholine, glutathione disulfide, and aspartate) were significantly increased in the everolimus-treated group, while 7 small molecules (lactate, alanine, arginine, glycine, formate, phosphorylcholine, and xanthine) were significantly decreased in the everolimus-treated group (Table 1).

Second, the metabolite profiles of sorafenib-treated HepG2 cells were markedly differentiated from combination therapy-treated HepG2 cells (Table 2). Two small molecules (glycerophosphorylcholine and uridine) were significantly increased in the combination therapy-treated group, while 12 small molecules (leucine, lactate, alanine, arginine, pyruvate, glycine, histidine, formate, trimethylamine, phosphorylcholine, xanthine, and hypoxanthine) were significantly decreased in the combination therapy-treated group (Table 2).

Third, the metabolite profiles of everolimus-treated HepG2 cells were markedly differentiated from combination therapy-treated HepG2 cells (Table 3). Three small molecules (arginine, xanthine, and hypoxanthine) were significantly increased in the combination therapy-treated group, while 10 small molecules (valine, lysine, β-glucose, uracil, tyrosine, glutathione disulfide, aspartate, glycerophosphorylcholine, and uridine) were significantly decreased in the combination therapy-treated group (Table 3).

Pathway analysis

First, in order of impact rank, the following pathways were significantly perturbed in the sorafenib monotherapy *vs.* everolimus monotherapy comparison (Figure 3A): (i) alanine, aspartate and glutamate metabolism (p=0.0059183), (ii) glycine, serine, and threonine metabolism (p=0.022631), (iii) methane metabolism (p=0.011701), (iv) pyruvate metabolism (p=0.010403), (v) pyrimidine metabolism (p=0.034351), (vi) aminoacyl-tRNA biosynthesis (p=3.56E-04), and (vii) glycerophospholipid metabolism (p=0.015242).

Second, in order of impact rank, the following pathways were significantly perturbed in the sorafenib monotherapy *vs.* combination therapy comparison (Figure 3B): pyruvate metabolism (p=7.04E-04), glycine, serine, and threonine metabolism (p=0.030424, methane metabolism (p=8.43E-04), glyoxylate and dicarboxylate metabolism (p=0.032822), glycolysis or gluconeogenesis (p=0.013269), alanine, aspartate, and glutamate metabolism (p=0.0080614), glycerophospholipid metabolism (p=0.020591), taurine and hypotaurine metabolism (p=0.0056238), purine metabolism (p=0.014483), and valine, leucine, and isoleucine biosynthesis (p=0.01015).

Indexed in: [Current Contents/Clinical Medicine] [SCI Expanded] [ISI Alerting System] [ISI Journals Master List] [Index Medicus/MEDLINE] [EMBASE/Excerpta Medica] [Chemical Abstracts/CAS] [Index Copernicus]

Table 2. Key metabolites responsible for discrimination between sorafenib monotherapy and sorfenib-everolimus combination therapy.

No.	Chemical shift/ppm multiplicity*	Metabolites	r**	*P*-value***
1	0.96(d), 1.68(m),1.71(m), 3.74(t)	Leucine	–0.342	1.015E-19
2	1.33(d), 4.11(q)	Lactate	–0.327	1.209E-8
3	1.48(d), 3.78(q)	Alanine	–0.287	6.683E-20
4	1.73(m), 1.93(m), 3.75(t)	Arginine	–0.972	3.572E-16
5	2.38(s)	Pyruvate	–0.622	1.134E-18
6	3.57(s)	Glycine	–0.555	2.450E-19
7	3.14(dd), 3.99(dd), 7.08(s)	Histidine	–0.285	7.043E-20
8	8.46(s)	Formate	–0.303	5.711E-20
9	2.88(s)	Trimethylamine	–0.434	7.043E-20
10	3.22(s), 3.61(t), 4.19(t)	Phosphorylcholine	–0.356	2.984E-15
11	3.23(s), 3.68(t), 4.32(t)	Glycerophosphorylcholine	0.354	8.235E-14
12	3.81(d), 4.14(q), 4.24(t), 5.90(d)	Uridine	0.443	1.201E-14
13	7.9(s)	Xanthine	–0.814	3.557E-20
14	8.2(s), 8.22(s)	Hypoxanthine	–0.234	1.372E-15

* Multiplicity: s – singlet; d – doublet; t – triplet; q – quartet; dd – doublet of doublets; m – multiplet. ** Correlation coefficient was obtained from OPLS-DA with a threshold of 0.226. Positive values indicate higher levels with sorafenib-everolimus treatment, and negative values indicate lower levels with sorafenib-everolimus treatment. *** *P*-values were derived from a non-parametric Mann-Whitney U test. The *p*-values of some main metabolites were not significantly perturbed in the univariate statistical analysis. But the OPLS-DA model showed that the addition of these metabolites resulted in the highest discrimination power. This result shows the advantage of a multivariate statistical approach in detecting the potential significance of subtle metabolic differences between experimental groups related to an associated univariate analysis.

Third, in order of impact rank, the following pathways were significantly perturbed in the everolimus monotherapy *vs.* combination therapy comparison (Figure 3C): aminoacyl-tRNA biosynthesis (p=1.72E-05), lysine biosynthesis (p=0.010403), and pyrimidine metabolism (p=0.034351).

Discussion

The efficacy of sorafenib has been well-established and is currently the standard of care for advanced HCC [15–17]. Mechanistically, sorafenib was originally developed to disrupt Raf/MEK/ERK signaling by inhibiting MEK and ERK phosphorylation; later research showed that sorafenib inhibits other receptor tyrosine kinases (e.g., vascular endothelial growth factor receptor (VEGFR)-2,3, platelet-derived growth factor receptor (PDGFR)-β, Fms-like tyrosine kinase 3 (FLT-3), and fibroblast growth factor receptor (FGFR)-1), as well as signal transducer and activator of transcription (STAT)-3 signaling [18]. Metabolically, Zhou et al. study in HepG2 cells showed that low-dose sorafenib treatment affects glycerophospholipid metabolism, while high-dose sorafenib treatment affects purine metabolism with significant decreases in GTP levels after sorafenib treatment [6].

Recent clinical trial-based evidence suggests that sorafenib combined with the mTOR inhibitor everolimus can be a more effective and tolerable treatment strategy for advanced HCC [2]. However, no study has yet comparatively assessed the metabolic effects of sorafenib, everolimus, and sorafenib-everolimus combination therapy on HCC cells. Therefore, in the present study we comparatively profiled the metabolite composition of HepG2 cells treated with sorafenib monotherapy, everolimus monotherapy, and sorafenib-everolimus combination therapy using a 2D HRMAS ^{1}H-NMR metabolomic approach, with all 3 OPLS-DA models displaying good separation between the experimental groups, high-quality goodness of fit (R2), and high-quality goodness of predication (Q2). First, we found that sorafenib and everolimus have differential metabolic effects on HepG2 cells with particular respect to amino acid, methane, pyruvate, pyrimidine, aminoacyl-tRNA biosynthesis, and glycerophospholipid metabolism. Moreover, we found that the addition of everolimus to sorafenib resulted in differential metabolic effects on HepG2 cells with particular respect to pyruvate, amino acid, methane, glyoxylate and dicarboxylate, glycolysis or gluconeogenesis, glycerophospholipid, and purine metabolism.

Indexed in: [Current Contents/Clinical Medicine] [SCI Expanded] [ISI Alerting System] [ISI Journals Master List] [Index Medicus/MEDLINE] [EMBASE/Excerpta Medica] [Chemical Abstracts/CAS] [Index Copernicus]

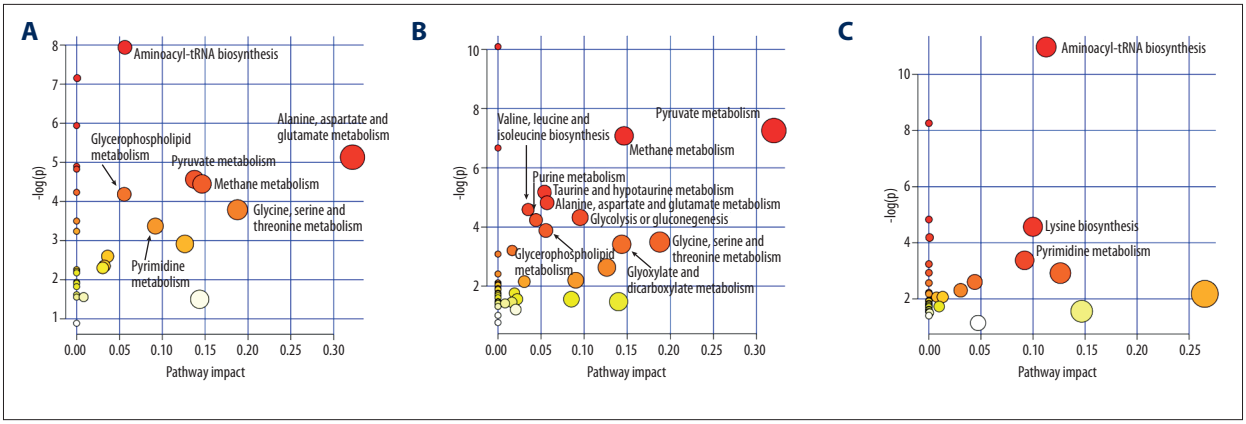

Figure 3. Pathway analysis. Plots depicting computed metabolic pathways as a function of -log (p) and pathway impact for the key differential metabolites from (**A**) sorafenib monotherapy (5 μM) *vs.* everolimus monotherapy (5 μM), (**B**) sorafenib monotherapy (5 μM) *vs.* combination therapy (5 μM sorafenib +5 μM everolimus), and (**C**) everolimus monotherapy (5 μM) *vs.* combination therapy (5 μM sorafenib +5 μM everolimus).

Table 3. Key metabolites responsible for discrimination between everolimus monotherapy and sorfenib-everolimus combination therapy.

No.	Chemical shift/ppm multiplicity*	Metabolites	r**	*P*-value***
1	0.99(d), 1.04(d), 2.25(m)	Valine	–0.404	1.432E-15
2	l.47(m), 1.73(m), 3.04(t), 3.76(t)	Lysine	–0.300	2.068E-14
3	1.73(m), 1.93(m), 3.75(t)	Arginine	0.596	8.873 E-1
4	4.27(d)	β-glucose	–0.254	2.448E-9
5	5.81(d), 7.54(d)	Uracil	–0.252	1.499E-14
6	3.06(dd), 3.94(dd), 6.91(d), 7.20(d)	Tyrosine	–0.399	9.656E-11
7	2.97(dd), 3.31(dd), 4.76(t)	Glutathionedisulfide	–0.378	4.407E-17
8	2.68(m), 2.82(m), 3.91(m)	Aspartate	–0.962	1.301E-15
9	3.23(s), 3.68(t), 4.32(t)	Glycerophosphorylcholine	–0.869	6.966E-16
10	3.81(d), 4.14(q), 4.24(t), 5.90(d)	Uridine	–0.415	5.124E-17
11	7.9(s)	Xanthine	0.379	6.181E-7
12	8.2(s), 8.22(s)	Hypoxanthine	0.301	2.876E-5

* Multiplicity: s – singlet; d – doublet; t – triplet; q – quartet; dd – doublet of doublets; m – multiplet. ** Correlation coefficient was obtained from OPLS-DA with a threshold of 0.226. Positive values indicate higher levels with sorafenib-everolimus treatment, and negative values indicate lower levels with sorafenib-everolimus treatment. *** *P*-values were derived from non-parametric Mann-Whitney U test. The *p*-values of some main metabolites were not significantly perturbed in the univariate statistical analysis. But the OPLS-DA model showed that the addition of these metabolites resulted in the highest discrimination power. This result shows the advantage of a multivariate statistical approach in detecting the potential significance of subtle metabolic differences between experimental groups related to an associated univariate analysis.

Therefore, combining the present findings with Zhou et al. previous findings suggests that the addition of everolimus therapy to first-line sorafenib therapy results in more pronounced metabolic changes to pyruvate, amino acid, methane, glyoxylate and dicarboxylate, and glycolysis or gluconeogenesis in HCC cells. This hypothesis is consistent with previous findings by Bradshaw-Pierce et al. that revealed everolimus' significant inhibition of glucose metabolism (decreases in lactate and glycolytic metabolites) in the colon tumor cell lines HT29 and HCT116. Based on this evidence, it appears that sorafenib therapy preferentially targets glycerophospholipid and purine metabolism, while the addition of everolimus therapy preferentially affects pyruvate, amino acid, and glucose metabolism in HCC cells. This phenomenon may explain

Indexed in: [Current Contents/Clinical Medicine] [SCI Expanded] [ISI Alerting System] [ISI Journals Master List] [Index Medicus/MEDLINE] [EMBASE/Excerpta Medica] [Chemical Abstracts/CAS] [Index Copernicus]

(in part) the synergistic effects of sorafenib-everolimus combination therapy observed *in vivo* [8]. This hypothesis differs from Piguet et al. suggestion that sorafenib-everolimus combination therapy synergistically reduces *in vivo* HCC tumor growth through sorafenib-induced HCC tumor cell apoptosis combined with everolimus-based inhibition of mTOR signaling in hepatic endothelial cells [8,19]. As this study only included HepG2 HCC cells (and not endothelial cells), we propose that sorafenib and everolimus may synergistically act on the metabolism of HCC tumor cells themselves in addition to separately acting on HCC cells and supporting endothelial cells, respectively (as Piguet et al. suggest). Further research applying sorafenib-everolimus combination therapy to both HCC tumor cells and surrounding cells is required to better understand its synergistic mode of action in HCC.

There are several limitations to this study. First, only 1 HCC cell line – HepG2 – was used in this study. The inclusion of more HCC cells lines would have provided additional validation for our findings. Second, we only used 1 set of dosing regimens based on a 5-μM dose for each treatment. The addition of more dosing regimens would have provided additional insights regarding dose-dependent effects but would have been cost-prohibitive. Third, we only employed 1 NMR-based metabolomic platform here. The addition of additional metabolomic platforms may have provided additional metabolite data for analysis but would have been cost-prohibitive.

Conclusions

In conclusion, sorafenib and everolimus have differential metabolic effects on HepG2 cells. It appears that sorafenib therapy preferentially targets glycerophospholipid and purine metabolism, while the addition of everolimus therapy preferentially affects pyruvate, amino acid, and glucose metabolism in HCC cells. This phenomenon may explain (in part) the synergistic effects of sorafenib-everolimus combination therapy observed *in vivo*. Further research on sorafenib-everolimus combination therapy is required to better understand its synergistic mode of action in HCC.

Acknowledgments

We thank Guoqing Ji at the Institutes of Biomedical Sciences at Fudan University for his helpful comments on this manuscript.

Statement

The funders had no role in study design, in the collection, analysis and interpretation of data, in the writing of the report, or the decision to submit the article for publication.

References:

1. Peixoto RDA, Renouf DJ, Gill S et al: Relationship of ethnicity and overall survival in patients treated with sorafenib for advanced hepatocellular carcinoma. J Gastrointest Oncol, 2014; 5: 259–64
2. Abdel-Rahman O, Fouad M: Sorafenib-based combination as a first line treatment for advanced hepatocellular carcinoma: a systematic review of the literature. Crit Rev Oncol Hematol, 2014; 91(1): 1–8
3. Bayet-Robert M, Loiseau D, Rio P et al: Quantitative two-dimensional HRMAS ^{1}H-NMR spectroscopy-based metabolite profiling of human cancer cell lines and response to chemotherapy. Magn Reson Med, 2010; 63: 1172–83
4. Pereira DSA, El-Bacha T, Kyaw N et al: Inhibition of energy-producing pathways of HepG2 cells by 3-bromopyruvate1. Biochem J, 2009; 417: 717–26
5. Liu X, Zhang C-c, Liu Z et al: LC-based targeted metabolomics analysis of nucleotides and identification of biomarkers associated with chemotherapeutic drugs in cultured cell models. Anticancer Drugs, 2014; 25: 690–703
6. Zhou S, Luo R: Metabolomic response to sorafenib treatment in human hepatocellular carcinoma cells. FASEB J, 2013; 27: 663–67
7. Bradshaw-Pierce EL, Pitts TM, Kulikowski G et al: Utilization of quantitative *in vivo* pharmacology approaches to assess combination effects of everolimus and irinotecan in mouse xenograft models of colorectal cancer. PloS One, 2013; 8: e58089
8. Piguet A-C, Saar B, Hlushchuk R et al: Everolimus augments the effects of sorafenib in a syngeneic orthotopic model of hepatocellular carcinoma. Mol Cancer Ther, 2011; 10: 1007–17
9. Li Y, Man S, Li J et al: The antitumor effect of formosanin C on HepG2 cell as revealed by ^{1}H-NMR based metabolic profiling. Chem Biol Interact, 2014; 220: 193–99
10. Massimi M, Tomassini A, Sciubba F et al: Effects of resveratrol on HepG2 cells as revealed by ^{1}H-NMR based metabolic profiling. Biochim Biophys Acta, 2012; 1820(1): 1–8
11. Bylesjö M, Rantalainen M, Cloarec O et al: OPLS discriminant analysis: combining the strengths of PLS-DA and SIMCA classification. J Chemom, 2006; 20: 341–51
12. Cloarec O, Dumas ME, Trygg J et al: Evaluation of the orthogonal projection on latent structure model limitations caused by chemical shift variability and improved visualization of biomarker changes in 1H NMR spectroscopic metabonomic studies. Anal Chem, 2005; 77: 517–26
13. Mahadevan S, Shah SL, Marrie TJ, Slupsky CM: Analysis of metabolomic data using support vector machines. Anal Chem, 2008; 80: 7562–70
14. Xia J, Mandal R, Sinelnikov IV et al: MetaboAnalyst 2.0 – a comprehensive server for metabolomic data analysis. Nucleic Acid Res, 2012; 40: W127–33
15. Llovet JM, Ricci S, Mazzaferro V et al: Sorafenib in advanced hepatocellular carcinoma. New Engl J Med, 2008; 359: 378–90
16. Cheng A-L, Kang Y-K, Chen Z et al: Efficacy and safety of sorafenib in patients in the Asia-Pacific region with advanced hepatocellular carcinoma: a phase III randomised, double-blind, placebo-controlled trial. Lancet Oncol, 2009; 10: 25–34
17. Lencioni R, Kudo M, Ye SL et al: First interim analysis of the GIDEON (Global Investigation of therapeutic decisions in hepatocellular carcinoma and of its treatment with sorafeNib) non-interventional study. Int J Clin Practic, 2012; 66: 675–83
18. Hung M-H, Tai W-T, Shiau C-W, Chen K-F: Downregulation of signal transducer and activator of transcription 3 by sorafenib: A novel mechanism for hepatocellular carcinoma therapy. World J Gastroenterol, 2014; 20: 15269–74
19. Ibrahim N, Yu Y, Walsh WR, Yang J-L: Molecular targeted therapies for cancer: Sorafenib monotherapy and its combination with other therapies (Review). Oncol Rep, 2012; 27: 1303–11

Indexed in: [Current Contents/Clinical Medicine] [SCI Expanded] [ISI Alerting System] [ISI Journals Master List] [Index Medicus/MEDLINE] [EMBASE/Excerpta Medica] [Chemical Abstracts/CAS] [Index Copernicus]